## Supplemental Data

# SIRT1 regulates metabolism and leukemogenic potential in CML stem cells

Ajay Abraham, Shaowei Qiu, Balu K. Chacko, Hui Li, Andrew Paterson, Jianbo He, Puneet Agarwal, Mansi Shah, Robert Welner, Victor M Darley-Usmar, Ravi Bhatia

## Supplemental Figure Legends

**Supplementary Figure 1.**

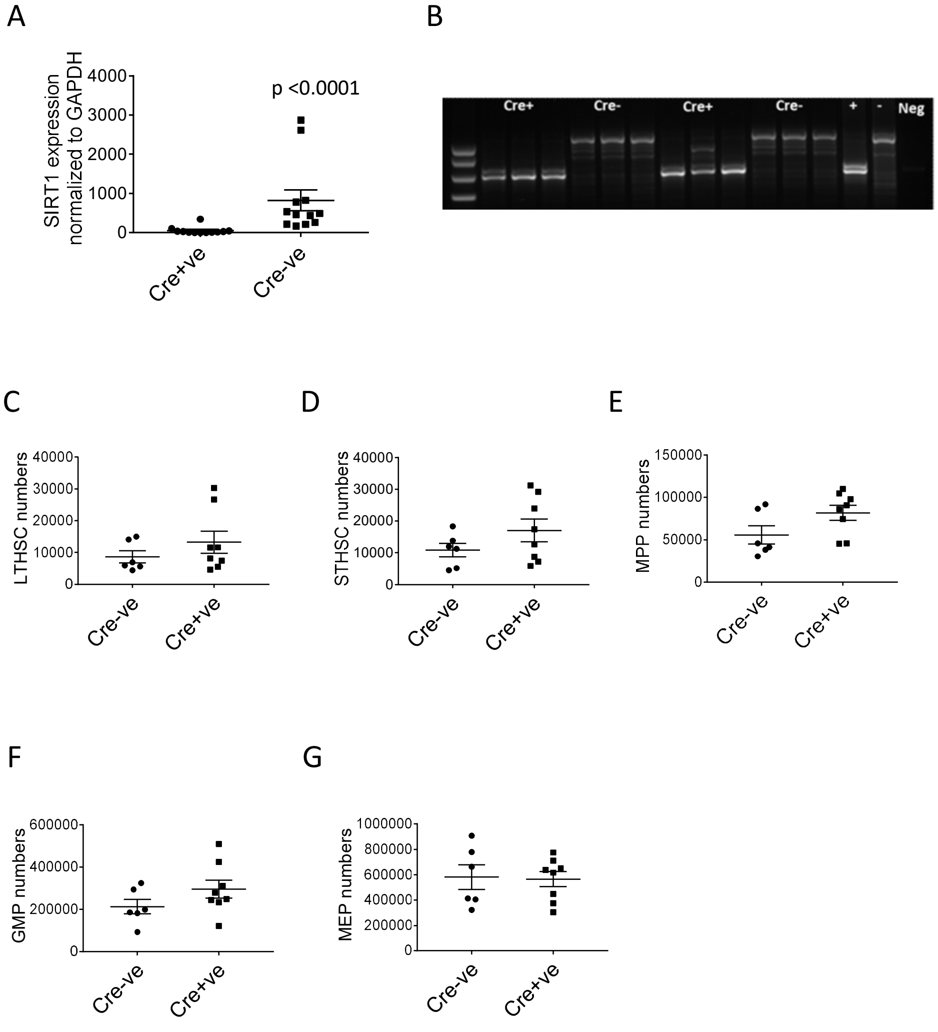

## Supplementary Figure 1 (related to Figure 1)

(A) Q-RT-PCR for SIRT1 expression in whole BM cells from Cre+ve and Cre-ve mice. (B) Genomic DNA PCR for SIRT1 excision, checked 2 weeks post pIpC induction. Results of transplantation of

BM cells into secondary recipients (n=8). Absolute numbers of BM LTHSC (C), STHSC (D), MPP (E), GMP (F) and MEP (G) 20 weeks post-secondary transplant.

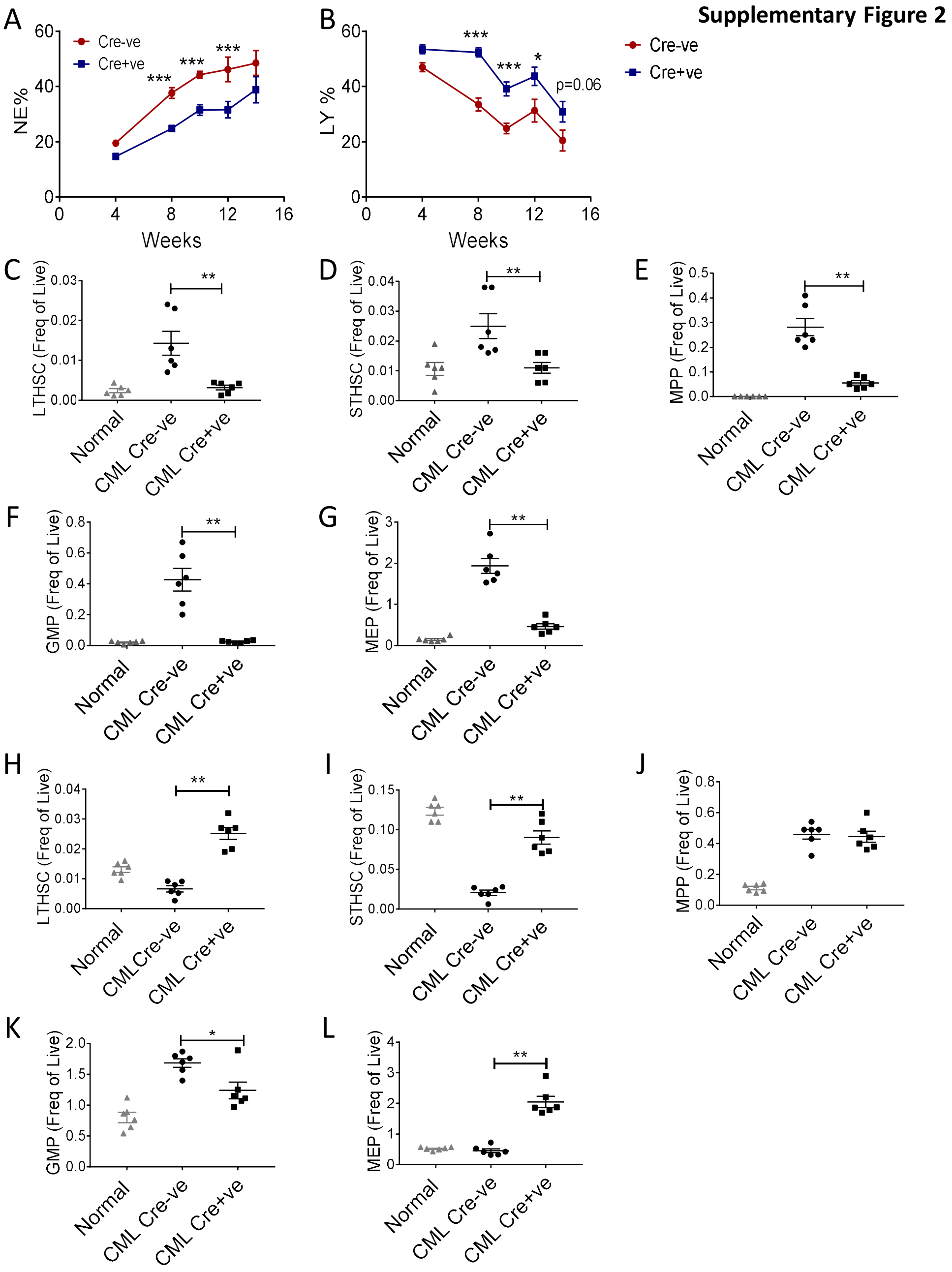

**Supplementary Figure 2 (related to Figure 3)**

(A) Neutrophil percentage and (B) Percentage of CD19+B220+ B cells in Cre-ve and Cre+ve CML mice. (C-G) Frequencies of splenic stem and progenitor sub-populations (LTHSC, STHSC, MPP, GMP and MEP) 8 weeks after CML induction and SIRT1 deletion. (H-L) Frequencies of BM stem and progenitor sub-populations (LTHSC, STHSC, MPP, GMP and MEP) 8 weeks after CML induction and SIRT1 deletion. Corresponding stem and progenitor cell populations from normal mice are shown for comparison. Error bars represent mean ± SEM. *P <0.05, **P <0.01, ***P <0.001, using t-test.

**Supplementary Figure 3**

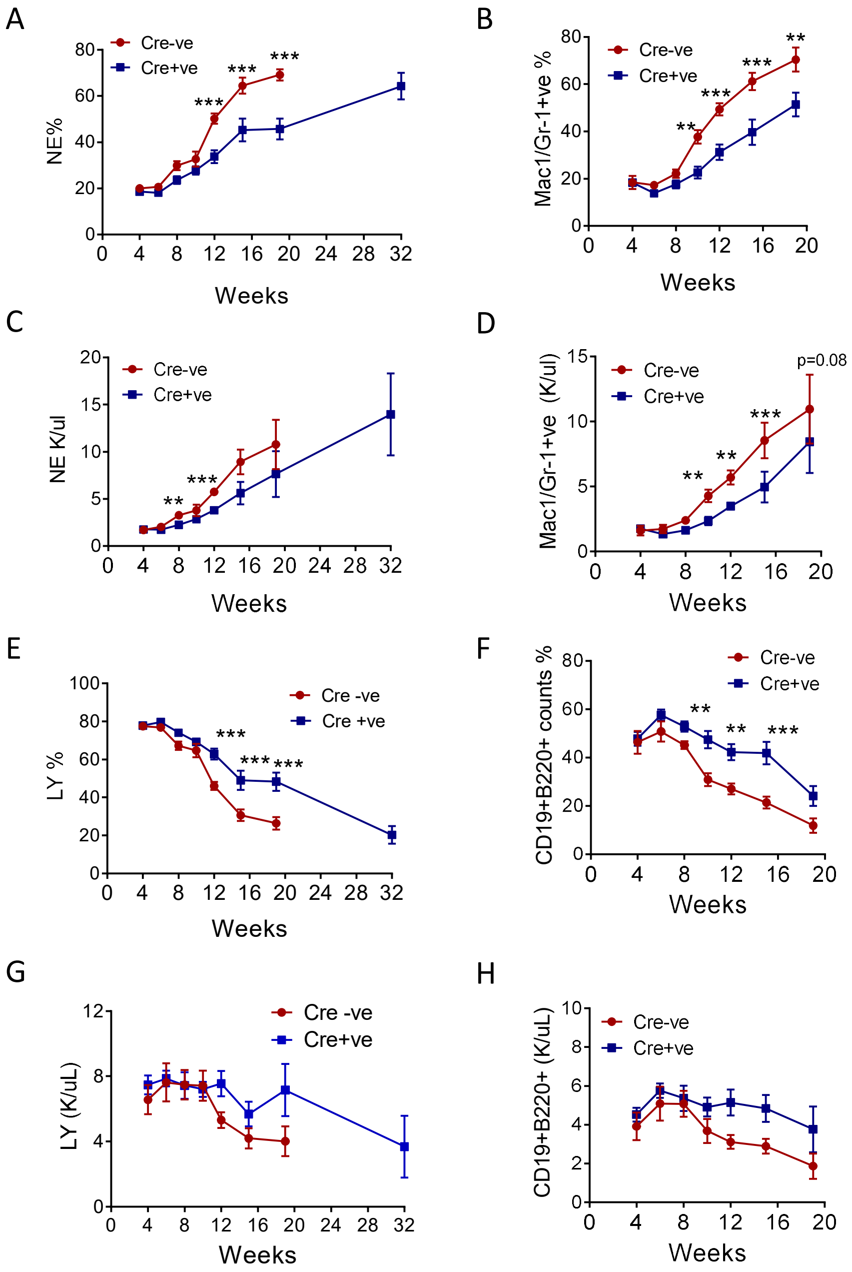

**Supplementary Figure 3 (related to Figure 3)**

Peripheral blood counts from primary Cre+ and Cre- mice followed for survival as shown in Figure 3T. (A) Neutrophil percentage, (B) absolute number of neutrophils, (C) Gr!+/Mac-1+ myeloid cell percentage, (D) absolute number of Gr1+/Mac-1+ myeloid cells, (E) lymphocyte percentage, (F) absolute number of lymphocytes, (G) CD19+/B220+ B cell percentage, (H) absolute number of CD19+/B220+ B cells, are shown. Error bars represent mean ± SEM. *P <0.05, **P <0.01, ***P <0.001, using t-tests.

**Supplementary Figure 4**

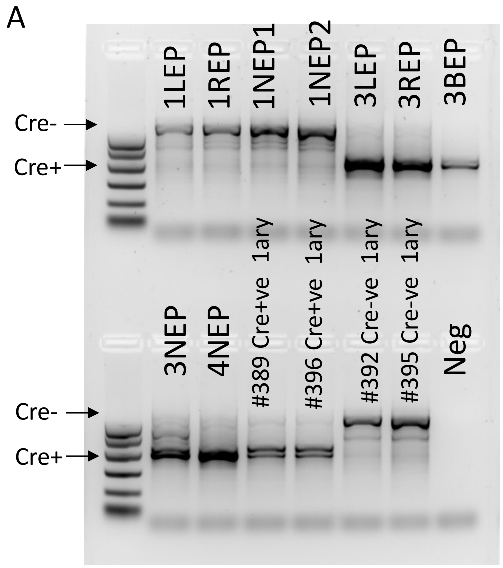

Blood Counts at 22 weeks CML (09/22/2016)

| | | WBC | NE | NE % | PLT |
|---|---|---|---|---|---|
| 1 LEP | Cre - | 19.18 | 10.54 | 54.94 | 3768 |
| 1 REP | Cre - | 8.38 | 4.75 | 56.71 | 3012 |
| 1 NEP1 | Cre - | 8.7 | 6.12 | 70.3 | 1113 |
| 1 NEP2 | Cre - | 18.54 | 6.79 | 36.6 | 1210 |
| 3 LEP | Cre+ | 11.14 | 4.47 | 40.1 | 237 |
| 3 REP | Cre+ | 10.76 | 6.33 | 58.85 | 3389 |
| 3 BEP | Cre+ | 3.1 | 1.41 | 45.49 | 168 |
| 3 NEP | Cre+ | 7.4 | 5.09 | 68.78 | 1049 |
| 4 NEP | Cre+ | 12.36 | 5.02 | 40.59 | 2368 |

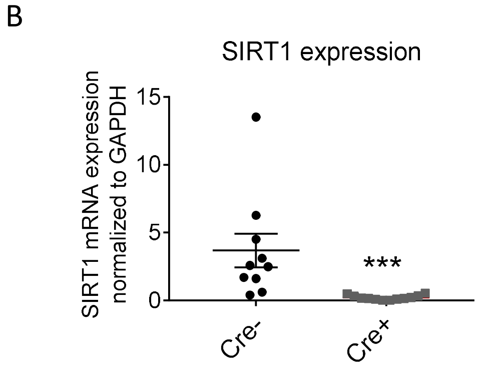

**Supplementary Figure 4 (related to Figure 3)**

(A) Genomic DNA PCR for SIRT1 excision, checked after 22 weeks post pIpC induction and CML induction to check SIRT1 deletion. (B) Q-RT-PCR for Sirt1 expression after 20 weeks post CML and pIpC induction. Error bars represent mean ± SEM. ***P <0.001, using t-test.

**Supplementary Figure 5**

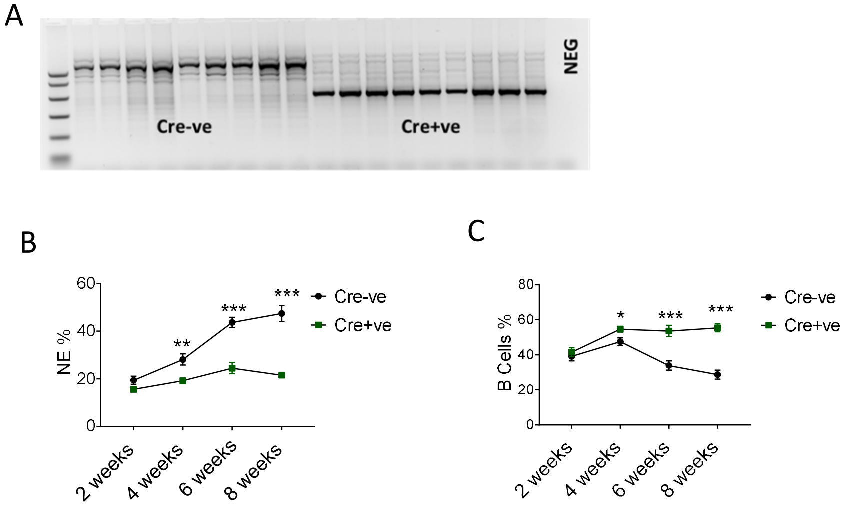

Spleen

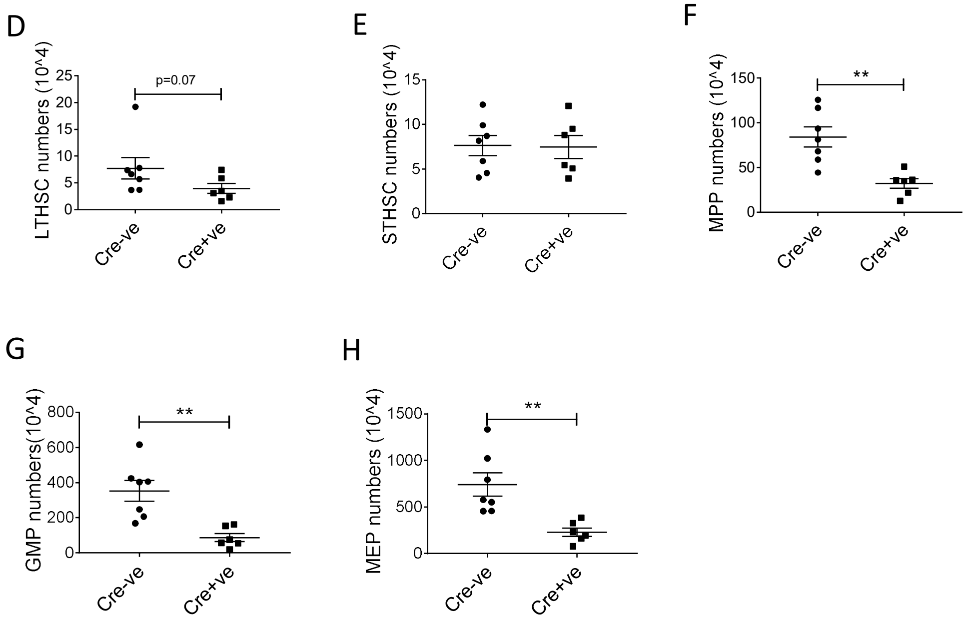

## Supplementary Figure 5 (related to Figure 4)

(A) Genomic DNA PCR for SIRT1 excision in the UBC ERT2-Cre/SIRT1$^{fl/fl}$/BCR-ABL model checked 2 weeks after Tamoxifen (TAM) administration. (B-C) Neutrophil (NE) percentages and donor derived B cells from peripheral blood of BA UBC ERT2-Cre SIRT1$^{fl/fl}$ or Cre-ve controls. (D-H)

Splenic stem and progenitor frequencies (LTHSC, STHSC, MPP, GMP and MEP) at 8 weeks post SIRT1 deletion and CML induction. Error bars represent mean ± SEM. *P <0.05, **P <0.01, ***P <0.001, using t-tests.

**Supplementary Figure 6**

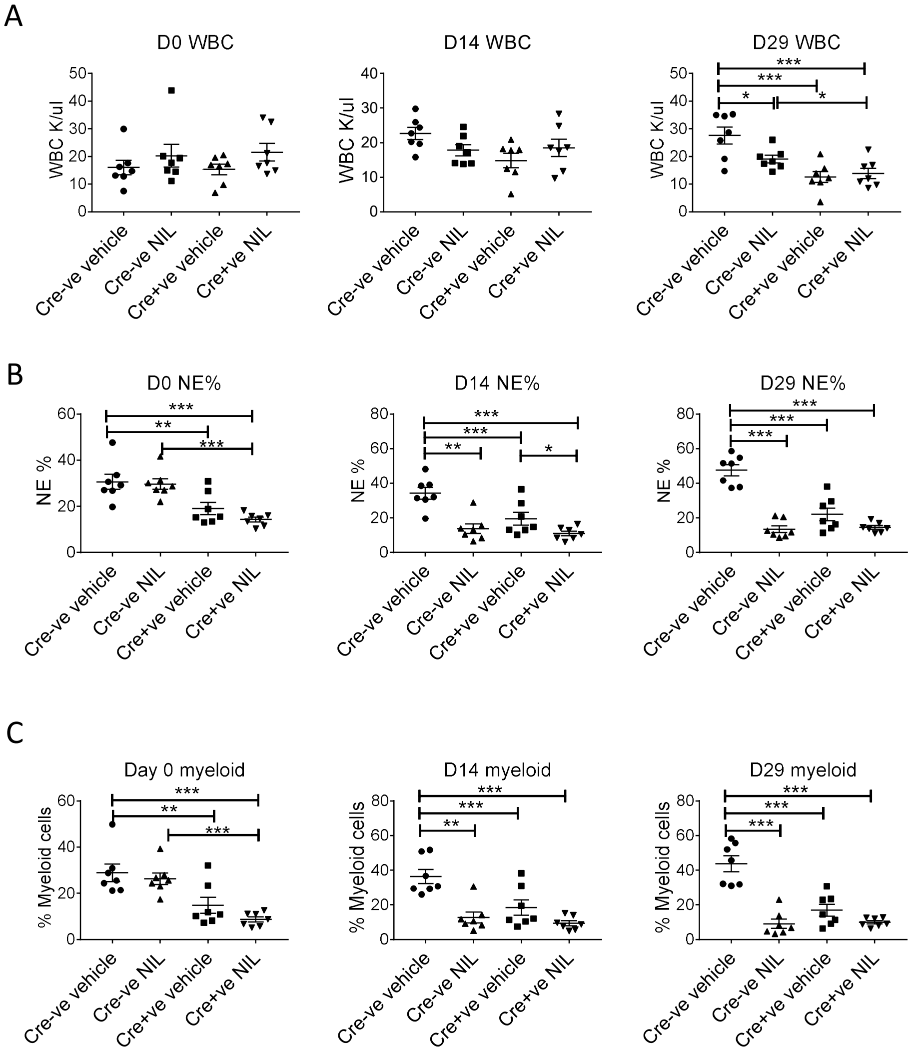

## Supplementary Figure 6 (related to Figure 5)

(A) Total WBC count, (B) Neutrophil (NE) % and (C) Gr1+/Mac1+ myeloid cells frequencies during Nilotinib (NIL) treatment. Error bars represent mean ± SEM. *P <0.05, **P <0.01, ***P <0.001, using ordinary one-way analysis of variance, correcting for multiple comparisons by controlling the False Discovery Rate using the two-stage linear step-up procedure of Benjamini, Krieger and Yekutieli.

**Supplementary Figure 7**

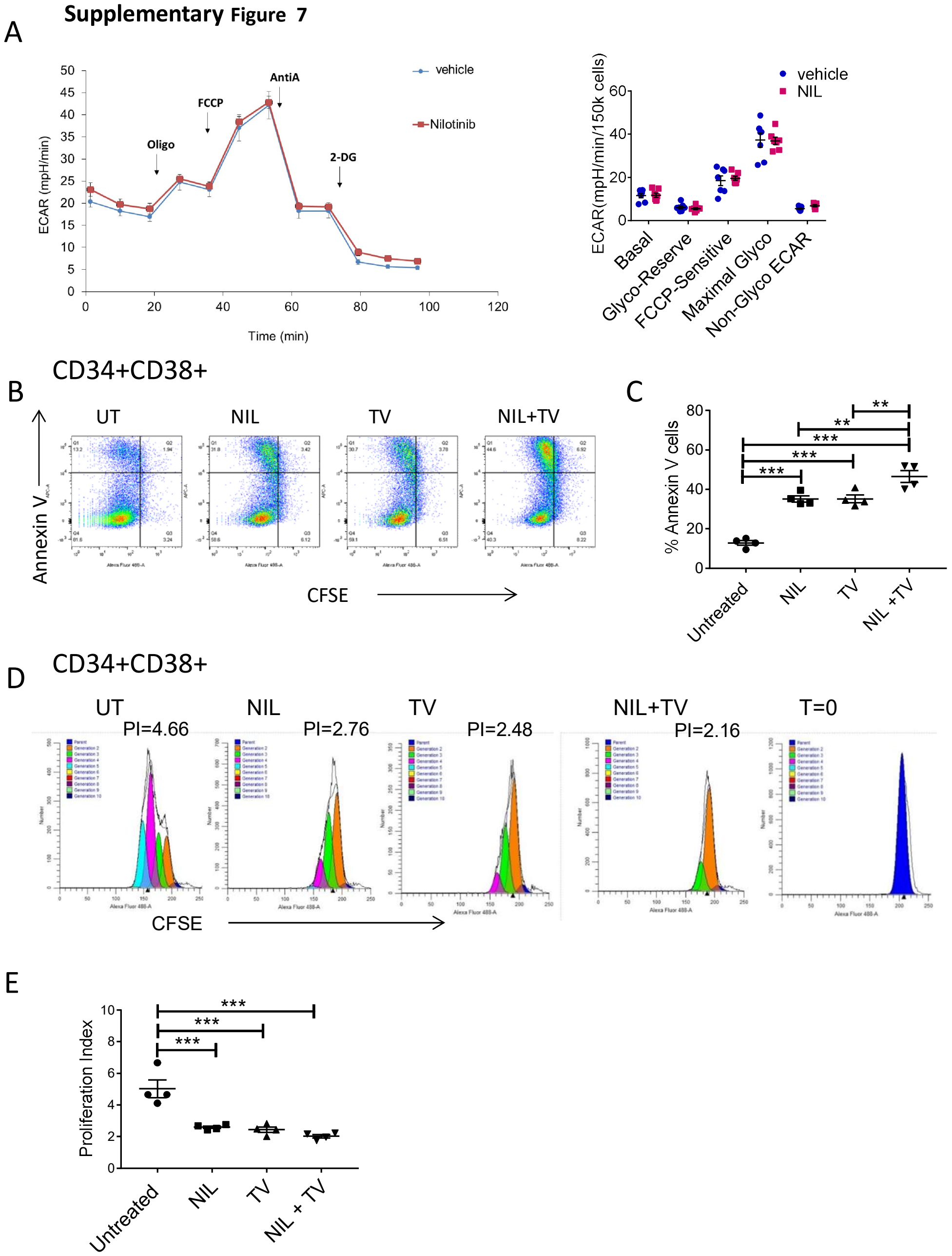

## Supplementary Figure 7 (related to Figure 8)

(A) ECAR measurements from c-Kit cells from CML mice treated with Nilotinib or vehicle (n=7 each) for 2 weeks (B) Representative flow cytometry plots showing Annexin V and CFSE expression for CML CP committed progenitors (CD34+CD38+) populations. (C) Apoptosis measured by Annexin V expression on CD34+CD38 cells. (D) Representative proliferation index plots generated using ModFit LT V5.09 after treating CML CD34+CD38+ cells with NIL or TV39OH or the combination. (E) Proliferation index measured based on analysis of CFSE plots on CML CD34+CD38+ cells. Error bars represent mean ± SEM. *P <0.05, **P <0.01, ***P <0.001, using ordinary one-way analysis of variance (C, E), and two-way analysis of variance (A), correcting for multiple comparisons by controlling the False Discovery Rate using the two-stage linear step-up procedure of Benjamini, Krieger and Yekutieli.

**Supplementary Figure 8**

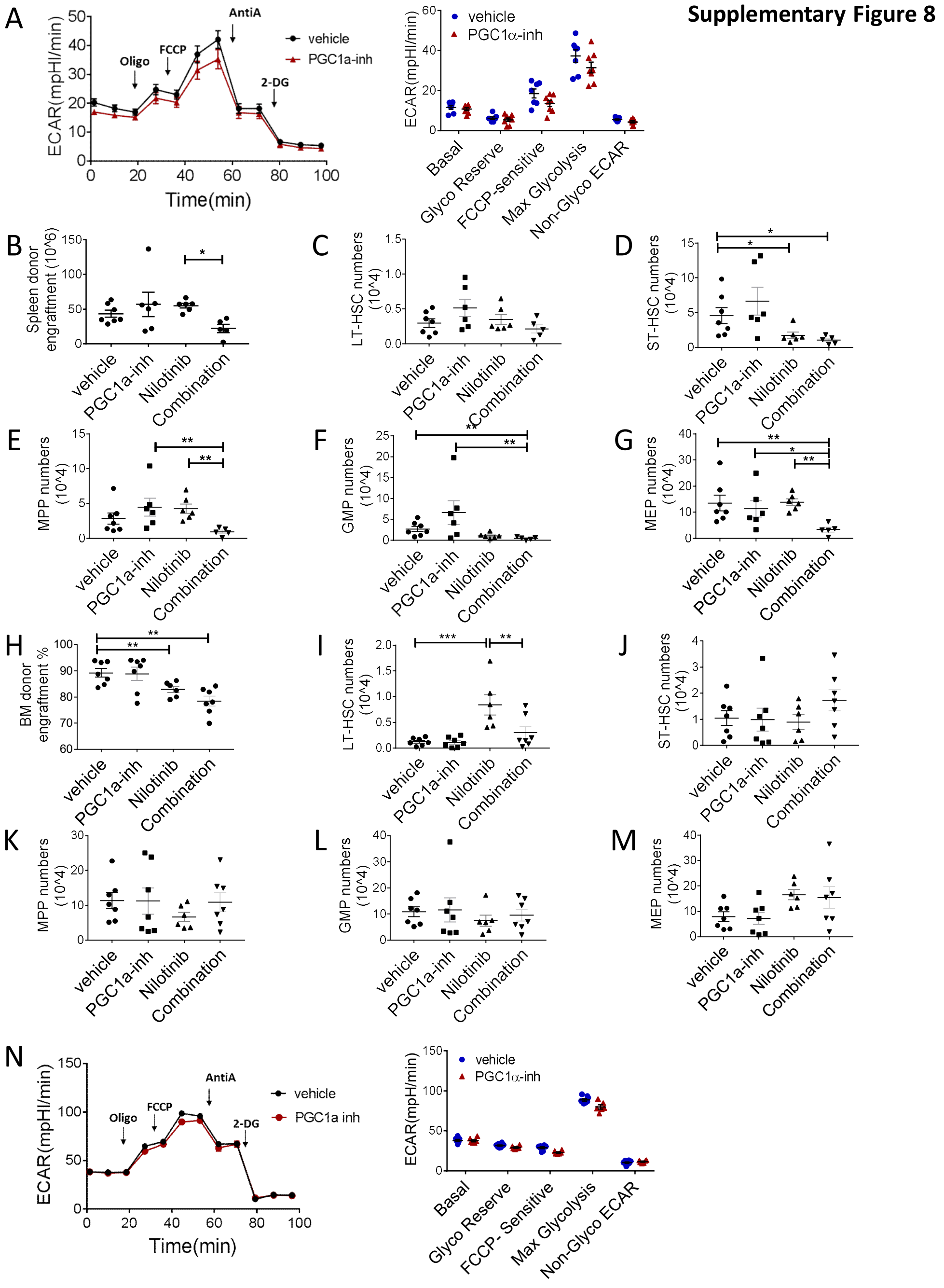

## Supplementary Figure 8 (related to Figure 9)

(A) ECAR measurements in c-Kit+ cells from CML mice treated with PGC1a inhibitor (SR18292) or vehicle (n=7 each) for 2 weeks. (B-F) Effect of vehicle, Nilotinib, SR18292 or the combination of Nilotinib and SR18292 on spleen donor cell engraftment percentage (B) and absolute number of

LT-HSC (C), ST-HSC (D), MPP (E), GMP (F) and MEP (G). (H-M) Effect of vehicle, Nilotinib, SR18292 and combination treatment on bone marrow donor cell engraftment percentage (H) and absolute number of LT-HSC (I), ST-HSC (J), MPP (K), GMP (L) and MEP (M). (N) ECAR measurement in CP CML CD34+ cells (n=3) treated overnight with SR18292 (40µM) or vehicle. Error bars represent mean ± SEM. *P <0.05, **P <0.01, ***P <0.001, using ordinary one-way analysis of variance (B-M), and two-way analysis of variance (A, N), correcting for multiple comparisons by controlling the False Discovery Rate using the two-stage linear step-up procedure of Benjamini, Krieger and Yekutieli.

**Supplementary Table 1**: Major down regulated gene signatures are shown with normalized enrichment scores (NES) and FDR q values.

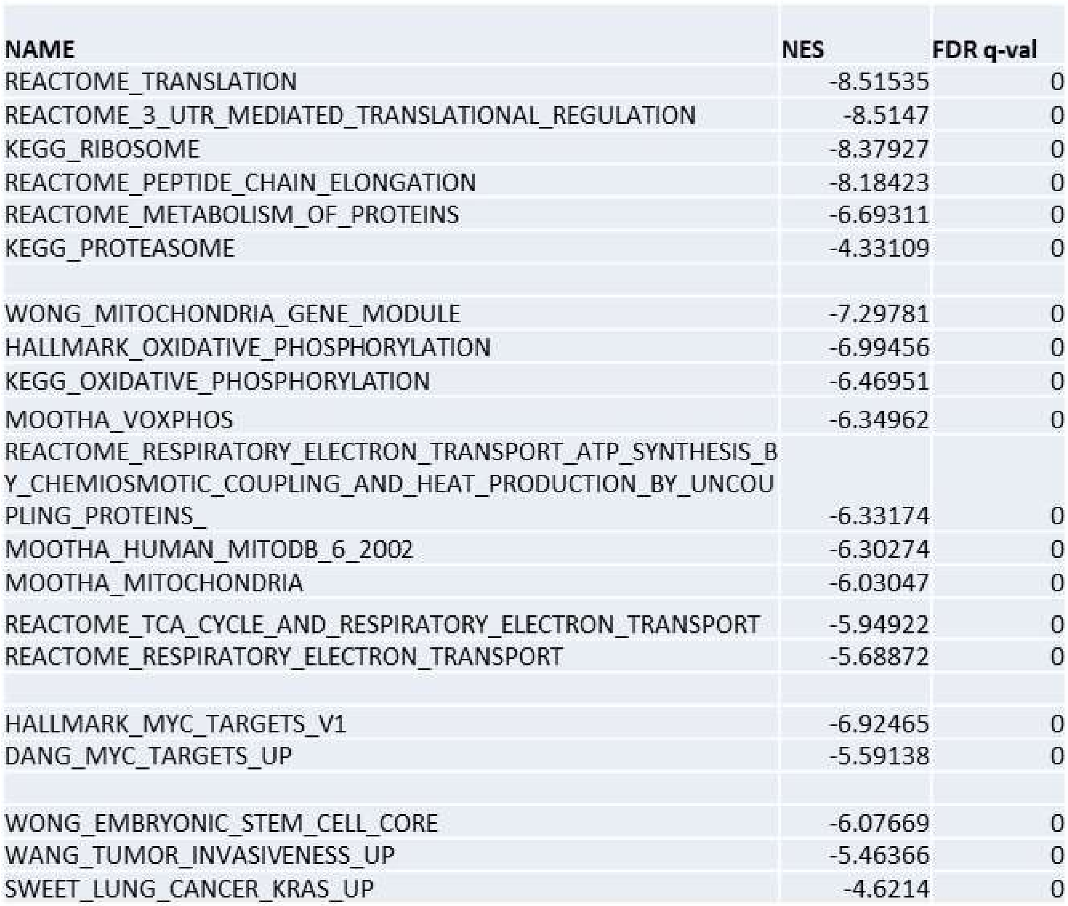

| NAME | NES | FDR q-val |
|---|---|---|
| REACTOME_TRANSLATION | -8.51535 | 0 |
| REACTOME_3_UTR_MEDIATED_TRANSLATIONAL_REGULATION | -8.5147 | 0 |
| KEGG_RIBOSOME | -8.37927 | 0 |
| REACTOME_PEPTIDE_CHAIN_ELONGATION | -8.18423 | 0 |
| REACTOME_METABOLISM_OF_PROTEINS | -6.69311 | 0 |
| KEGG_PROTEASOME | -4.33109 | 0 |
| | | |
| WONG_MITOCHONDRIA_GENE_MODULE | -7.29781 | 0 |
| HALLMARK_OXIDATIVE_PHOSPHORYLATION | -6.99456 | 0 |
| KEGG_OXIDATIVE_PHOSPHORYLATION | -6.46951 | 0 |
| MOOTHA_VOXPHOS | -6.34962 | 0 |
| REACTOME_RESPIRATORY_ELECTRON_TRANSPORT_ATP_SYNTHESIS_BY_CHEMIOSMOTIC_COUPLING_AND_HEAT_PRODUCTION_BY_UNCOUPLING_PROTEINS_ | -6.33174 | 0 |
| MOOTHA_HUMAN_MITODB_6_2002 | -6.30274 | 0 |
| MOOTHA_MITOCHONDRIA | -6.03047 | 0 |
| REACTOME_TCA_CYCLE_AND_RESPIRATORY_ELECTRON_TRANSPORT | -5.94922 | 0 |
| REACTOME_RESPIRATORY_ELECTRON_TRANSPORT | -5.68872 | 0 |
| | | |
| HALLMARK_MYC_TARGETS_V1 | -6.92465 | 0 |
| DANG_MYC_TARGETS_UP | -5.59138 | 0 |
| | | |
| WONG_EMBRYONIC_STEM_CELL_CORE | -6.07669 | 0 |
| WANG_TUMOR_INVASIVENESS_UP | -5.46366 | 0 |
| SWEET_LUNG_CANCER_KRAS_UP | -4.6214 | 0 |

**Supplementary Table 2:** Major upregulated gene signatures in SIRT1 deleted LSK cells. Normalized enrichment scores (NES) and FDR q values are shown.

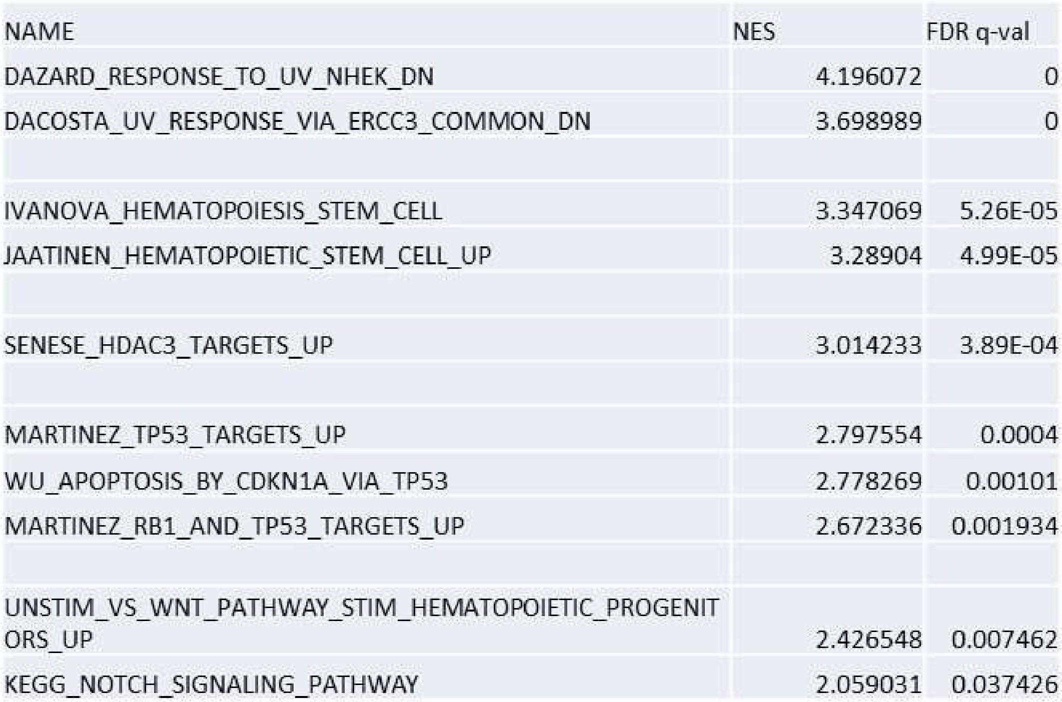

| NAME | NES | FDR q-val |
|---|---|---|
| DAZARD_RESPONSE_TO_UV_NHEK_DN | 4.196072 | 0 |
| DACOSTA_UV_RESPONSE_VIA_ERCC3_COMMON_DN | 3.698989 | 0 |
| | | |
| IVANOVA_HEMATOPOIESIS_STEM_CELL | 3.347069 | 5.26E-05 |
| JAATINEN_HEMATOPOIETIC_STEM_CELL_UP | 3.28904 | 4.99E-05 |
| | | |
| SENESE_HDAC3_TARGETS_UP | 3.014233 | 3.89E-04 |
| | | |
| MARTINEZ_TP53_TARGETS_UP | 2.797554 | 0.0004 |
| WU_APOPTOSIS_BY_CDKN1A_VIA_TP53 | 2.778269 | 0.00101 |
| MARTINEZ_RB1_AND_TP53_TARGETS_UP | 2.672336 | 0.001934 |
| | | |
| UNSTIM_VS_WNT_PATHWAY_STIM_HEMATOPOIETIC_PROGENITORS_UP | 2.426548 | 0.007462 |
| KEGG_NOTCH_SIGNALING_PATHWAY | 2.059031 | 0.037426 |

**Supplementary Table 3:** Top 100 GSEA signatures from CML vs normal LTHSC RNA analysis were compared with the corresponding GSEA signatures in SIRT1KO vs controls. Normalized enrichment scores (NES) were compared.

| SL No | NAME |
|---|---|
| 1 | STARK_PREFRONTAL_CORTEX_22Q11_DELETION_DN |
| 2 | WONG_MITOCHONDRIA_GENE_MODULE |
| 3 | HSIAO_HOUSEKEEPING_GENES |
| 4 | REACTOME_RESPIRATORY_ELECTRON_TRANSPORT_ATP_SYNTHESIS |
| 5 | REACTOME_METABOLISM_OF_MRNA |
| 6 | HALLMARK_OXIDATIVE_PHOSPHORYLATION |
| 7 | REACTOME_TRANSLATION |
| 8 | REACTOME_METABOLISM_OF_RNA |
| 9 | REACTOME_INFLUENZA_VIRAL_RNA_TRANSCRIPTION_AND_REPLICATION |
| 10 | GSE2405_0H_VS_24H_A_PHAGOCYTOPHILUM_STIM_NEUTROPHIL_UP |
| 11 | YAO_TEMPORAL_RESPONSE_TO_PROGESTERONE_CLUSTER_13 |
| 12 | KEGG_OXIDATIVE_PHOSPHORYLATION |
| 13 | REACTOME_PEPTIDE_CHAIN_ELONGATION |
| 14 | REACTOME_RESPIRATORY_ELECTRON_TRANSPORT |
| 15 | REACTOME_SRP_DEPENDENT_COTRANSLATIONAL_PROTEIN_TARGETING_TO_MEMBRANE |
| 16 | KEGG_RIBOSOME |
| 17 | MOOTHA_HUMAN_MITODB_6_2002 |
| 18 | MOOTHA_VOXPHOS |
| 19 | REACTOME_TCA_CYCLE_AND_RESPIRATORY_ELECTRON_TRANSPORT |
| 20 | REACTOME_3_UTR_MEDIATED_TRANSLATIONAL_REGULATION |
| 21 | KEGG_PARKINSONS_DISEASE |
| 22 | REACTOME_NONSENSE_MEDIATED_DECAY_ENHANCED_BY_THE_EXON_JUNCTION_COMPLEX |
| 23 | GSE2405_0H_VS_9H_A_PHAGOCYTOPHILUM_STIM_NEUTROPHIL_DN |
| 24 | REACTOME_METABOLISM_OF_PROTEINS |
| 25 | GSE26030_TH1_VS_TH17_RESTIMULATED_DAY5_POST_POLARIZATION_UP |
| 26 | YAO_TEMPORAL_RESPONSE_TO_PROGESTERONE_CLUSTER_17 |
| 27 | MOOTHA_MITOCHONDRIA |
| 28 | GSE3720_UNSTIM_VS_PMA_STIM_VD1_GAMMADELTA_TCELL_UP |
| 29 | WONG_EMBRYONIC_STEM_CELL_CORE |
| 30 | REACTOME_INFLUENZA_LIFE_CYCLE |
| 31 | KEGG_HUNTINGTONS_DISEASE |
| 32 | TAKAO_RESPONSE_TO_UVB_RADIATION_UP |
| 33 | DAIRKEE_TERT_TARGETS_UP |
| 34 | KAECH_DAY8_EFF_VS_DAY15_EFF_CD8_TCELL_UP |
| 35 | GSE14000_TRANSLATED_RNA_VS_MRNA_DC_DN |
| 36 | LI_AMPLIFIED_IN_LUNG_CANCER |
| 37 | REACTOME_VIF_MEDIATED_DEGRADATION_OF_APOBEC3G |
| 38 | REACTOME_ER_PHAGOSOME_PATHWAY |
| 39 | BILANGES_SERUM_AND_RAPAMYCIN_SENSITIVE_GENES |
| 40 | GSE24210_CTRL_VS_IL35_TREATED_TCONV_CD4_TCELL_DN |
| 41 | REACTOME_SCF_BETA_TRCP_MEDIATED_DEGRADATION_OF_EMI1 |
| 42 | KEGG_PROTEASOME |
| 43 | CHNG_MULTIPLE_MYELOMA_HYPERPLOID_UP |
| 44 | SWEET_LUNG_CANCER_KRAS_UP |
| 45 | REACTOME_CDK_MEDIATED_PHOSPHORYLATION_AND_REMOVAL_OF_CDC6 |
| 46 | REACTOME_AUTODEGRADATION_OF_THE_E3_UBIQUITIN_LIGASE_COP1 |
| 47 | REACTOME_REGULATION_OF_APOPTOSIS |
| 48 | REACTOME_CROSS_PRESENTATION_OF_SOLUBLE_EXOGENOUS_ANTIGENS_ENDOSOMES |
| 49 | HALLMARK_MYC_TARGETS_V1 |
| 50 | PECE_MAMMARY_STEM_CELL_UP |
| 51 | GSE26030_TH1_VS_TH17_RESTIMULATED_DAY15_POST_POLARIZATION_DN |
| 52 | KAECH_NAIVE_VS_DAY8_EFF_CD8_TCELL_DN |
| 53 | REACTOME_ANTIGEN_PROCESSING_CROSS_PRESENTATION |
| 54 | GSE22886_DAY1_VS_DAY7_MONOCYTE_IN_CULTURE_DN |
| 55 | REACTOME_P53_INDEPENDENT_G1_S_DNA_DAMAGE_CHECKPOINT |
| 56 | REACTOME_CDT1_ASSOCIATION_WITH_THE_CDC6_ORC_ORIGIN_COMPLEX |
| 57 | REACTOME_REGULATION_OF_ORNITHINE_DECARBOXYLASE_ODC |
| 58 | GSE45837_WT_VS_GFI1_KO_PDC_DN |
| 59 | REACTOME_DESTABILIZATION_OF_MRNA_BY_AUF1_HNRNP_D0 |
| 60 | GSE9509_10MIN_VS_30MIN_LPS_STIM_IL10_KO_MACROPHAGE_UP |
| 61 | GSE2770_UNTREATED_VS_ACT_CD4_TCELL_6H_UP |
| 62 | REACTOME_METABOLISM_OF_AMINO_ACIDS_AND_DERIVATIVES |
| 63 | GSE42724_NAIVE_VS_B1_BCELL_DN |
| 64 | REACTOME_APC_C_CDH1_MEDIATED_DEGRADATION |
| 65 | CHIANG_LIVER_CANCER_SUBCLASS_UNANNOTATED_DN |
| 66 | REACTOME_SCFSKP2_MEDIATED_DEGRADATION_OF_P27_P21 |
| 67 | GSE22886_NEUTROPHIL_VS_MONOCYTE_DN |
| 68 | REACTOME_REGULATION_OF_MRNA_STABILITY_BY_PROTEINS_THAT_BIND_AU_RICH_ELEMENTS |
| 69 | GSE39820_TGFBETA1_IL6_VS_TGFBETA1_IL6_IL23A_TREATED_CD4_TCELL_DN |
| 70 | GSE13547_2H_VS_12_H_ANTI_IGM_STIM_BCELL_DN |
| 71 | BIOCARTA_PROTEASOME_PATHWAY |
| 72 | REACTOME_P53_DEPENDENT_G1_DNA_DAMAGE_RESPONSE |
| 73 | ENK_UV_RESPONSE_KERATINOCYTE_UP |
| 74 | KAMIKUBO_MYELOID_CEBPA_NETWORK |
| 75 | KEGG_ALZHEIMERS_DISEASE |
| 76 | REACTOME_REGULATION_OF_MITOTIC_CELL_CYCLE |
| 77 | REACTOME_APC_C_CDC20_MEDIATED_DEGRADATION_OF_MITOTIC_PROTEINS |
| 78 | GSE3720_UNSTIM_VS_LPS_STIM_VD2_GAMMADELTA_TCELL_UP |
| 79 | GSE12845_IGD_NEG_BLOOD_VS_NAIVE_TONSIL_BCELL_UP |
| 80 | TARTE_PLASMA_CELL_VS_PLASMABLAST_DN |
| 81 | KAECH_DAY8_EFF_VS_MEMORY_CD8_TCELL_UP |
| 82 | GSE9650_EFFECTOR_VS_MEMORY_CD8_TCELL_UP |
| 83 | GSE7509_UNSTIM_VS_FCGRIIB_STIM_MONOCYTE_UP |
| 84 | GSE17721_PAM3CSK4_VS_CPG_12H_BMDC_UP |
| 85 | GSE14699_DELETIONAL_TOLERANCE_VS_ACTIVATED_CD8_TCELL_DN |
| 86 | BURTON_ADIPOGENESIS_6 |
| 87 | GSE13522_CTRL_VS_T_CRUZI_Y_STRAIN_INF_SKIN_BALBC_MOUSE_UP |
| 88 | GSE14000_TRANSLATED_RNA_VS_MRNA_4H_LPS_DC_DN |
| 89 | GSE26030_UNSTIM_VS_RESTIM_TH1_DAY5_POST_POLARIZATION_DN |
| 90 | REACTOME_ACTIVATION_OF_NF_KAPPAB_IN_B_CELLS |
| 91 | MOOTHA_PGC |
| 92 | GSE7831_UNSTIM_VS_INFLUENZA_STIM_PDC_1H_UP |
| 93 | GSE24142_ADULT_VS_FETAL_EARLY_THYMIC_PROGENITOR_DN |
| 94 | GSE21379_WT_VS_SAP_KO_TFH_CD4_TCELL_UP |
| 95 | REACTOME_ACTIVATION_OF_THE_MRNA_UPON_BINDING_OF_THE_CAP_BINDING_COMPLEX |
| 96 | GSE19888_ADENOSINE_A3R_ACT_VS_A3R_ACT_WITH_A3R_INH_PRETREATMENT_IN_MAST_CELL_UP |
| 97 | GSE14415_INDUCED_TREG_VS_FAILED_INDUCED_TREG_UP |
| 98 | GSE37532_TREG_VS_TCONV_CD4_TCELL_FROM_LN_UP |
| 99 | REACTOME_FORMATION_OF_THE_TERNARY_COMPLEX_AND_SUBSEQUENTLY_THE_43S_COMPLEX |
| 100 | GSE411_100MIN_VS_400MIN_IL6_STIM_MACROPHAGE_DN |